Journal of Science and Transport Technology
Journal homepage: https://jstt.vn/index.php/en

Investigation of the control system for air supply during transient operation of a turbocharged diesel engine

Vu Ngoc Khiem, Nguyen Van Tuan*, Tran Trong Tuan
School of Transportation Engineering, University of Transport Technology, No. 54 Trieu Khuc Street, Thanh Liet, Hanoi 100000, Vietnam

Article info
Type of article:
Original research paper

DOI:
https://doi.org/10.58845/jstt.utt.2026.en.6.1.87-100

***Corresponding author:**
Email address:
nguyenvantuan@utt.edu.vn

Received: 08/10/2025
Received in Revised Form: 20/12/2025
Accepted: 12/01/2026

Abstract: In the context of increasingly stringent emission standards and higher fuel efficiency requirements for turbocharged diesel engines, optimizing air-path control, particularly during transient operating conditions, has become essential. This study focuses on the design and evaluation of a dedicated air supply controller for transient operation to enhance the response and stability of a turbocharged diesel engine. The controller was developed to regulate the intake airflow dynamically through an auxiliary bypass line, compensating for turbocharger lag and maintaining stable boost pressure during rapid load or speed changes. Experimental results demonstrate that the proposed air supply controller significantly improves transient performance. Specifically, the transition time was reduced from 3 seconds to 1.5÷2 seconds, corresponding to an improvement of 16.6÷40%, while speed fluctuation Δn decreased by 8.5÷24%, depending on the load level. The best improvement was achieved at medium to high loads (50÷65%), indicating rapid and stable turbocharger response with the assistance of the supplemental air supply system. At low loads, the controller's impact was less pronounced due to lower boost pressure and airflow rates. The results confirm that the proposed air-path controller for transient operation is a feasible and effective solution to shorten transient response time, reduce speed fluctuation, improve engine stability, and potentially reduce emissions in turbocharged diesel engines operating under rapidly varying conditions.

Keywords: Turbocharged diesel engine, transient operation, air supply controller, transient response.

1. Introduction

As emission standards become increasingly stringent for internal combustion engines, various strategies have been developed to reduce exhaust emissions and improve fuel economy, including the use of alternative fuels, advanced combustion concepts, structural optimization, and exhaust aftertreatment systems [1-4]. Developing more effective control strategies for modern diesel engines remains essential for improving emission characteristics [5,6]. Modern diesel engines are commonly equipped with variable geometry turbochargers (VGT) and exhaust gas recirculation (EGR) systems [7-9]. Turbocharging helps to reduce fuel consumption, while EGR significantly decreases nitrogen oxide (NO_x) emissions [10-14]. Under increasingly stringent emission limits and higher fuel efficiency demands, particularly in

transportation, industrial, and power generation applications, air-path control during transient operation has become a key technological challenge [15-17]. During transitions between operating states such as load increase, load reduction, or speed variation, the turbocharger, EGR system, and intake/exhaust manifolds must quickly adjust to ensure sufficient air supply, stable boost pressure, and proper exhaust gas recirculation. However, due to factors such as turbocharger lag, gas flow inertia, and the dynamic characteristics of intake and exhaust systems, transient responses are often degraded, leading to reduced boost pressure, increased fuel-to-air ratios, higher smoke and NO_x emissions, and unstable engine speed, ultimately affecting performance and drivability [18,19].

Several studies have demonstrated that coordinated control of components such as the EGR valve, VGT, and wastegate, combined with adaptive or feedforward control strategies, can significantly enhance transient response [20-23]. Nevertheless, the air-path model during transient operation is inherently complex, involving interactions among flow rates, pressures, EGR, turbine dynamics, and sometimes even the thermal effects of the pipes and turbocharger [24,25]. Designing a controller that achieves fast transient response while maintaining stability in steady-state operation thus presents a challenging multi-objective problem.

Most existing research focuses on EGR/VGT coordination or multi-stage boosting control. At the same time, few studies specifically address the air supply controller for transient operation in turbocharged diesel engines, particularly under rapid load variation or real-world cyclic operation. The absence of an optimal control solution for the air-path system during transient conditions can lead to efficiency losses and uncontrolled emission increases.

Therefore, this study focuses on the design and implementation of a dedicated air supply control system for transient operation in a turbocharged diesel engine. The objective is to ensure timely and stable air delivery under varying load and speed conditions, thereby improving overall efficiency, reducing emissions, and enhancing engine stability, meeting the growing demands for cleaner and more efficient diesel engine technologies in modern industrial and transportation applications.

2. Theoretical Basis

2.1. Sudden Load Change Processes

A rapid change in load with a large variation intensity is called a sudden load change. In these processes, the engine's resisting torque increases or decreases (also referred to as load engagement or load disengagement), leading to a change in engine speed. The degree of speed variation depends on the quality and technical condition of the engine. Load engagement or disengagement should be carried out when the engine speed is close to the rated speed or at a low speed.

The most demanding operating condition for a turbocharged engine occurs when a large load is suddenly applied from the no-load condition, or when the engine speed increases rapidly due to an abrupt increase in the fuel throttle. To evaluate and compare the performance efficiency of different engines during load engagement or disengagement, it is necessary to use the same load engagement and disengagement characteristics for all engines, typically considering an instantaneous 100% load change. The two main criteria for evaluating the quality of the transition when the load changes are the relative rotation change, j, and the transition time, T_{ct}. The curves illustrating the change in engine speed during load engagement and disengagement are shown in Fig. 1 and Fig. 2. The relative speed variation φ is calculated based on the initial operating speed compared to the rated speed:

$$\varphi = \frac{\omega - \omega_{dm}}{\omega_{dm}} \quad (1)$$

The duration of the transient process is

calculated from the moment the load change begins to the moment when the engine speed starts to oscillate steadily within the tolerance band ψ. When the engine operates along the governor characteristic corresponding to the rated speed, with constant load modes and no-load mode, the instability degree ψ is within 1%, meaning the engine speed is allowed to fluctuate within ±0.5% of the average value. To prevent short-term engine overspeed during sudden load changes, the relative speed variation φ must not exceed 10–12%. For engines driving alternating current generators, when subjected to sudden load changes, φ should be maintained within 5–6%. Another essential characteristic is the rate of damping of oscillations. The duration of the transient process (T_{ct}) is typically limited to 5–10 seconds.

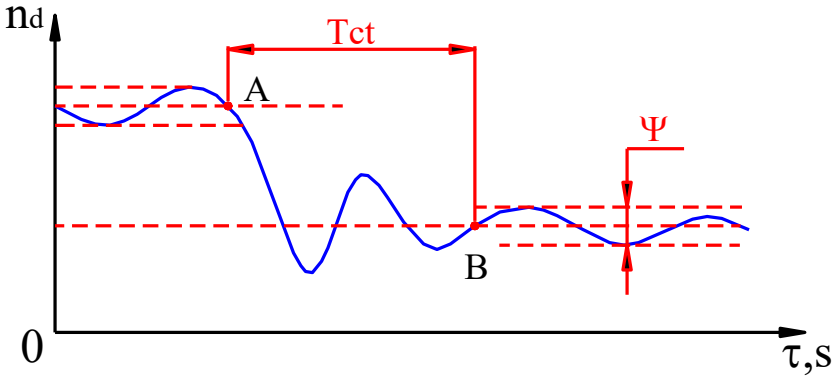

Fig. 1. Transient process of the engine during sudden load engagement

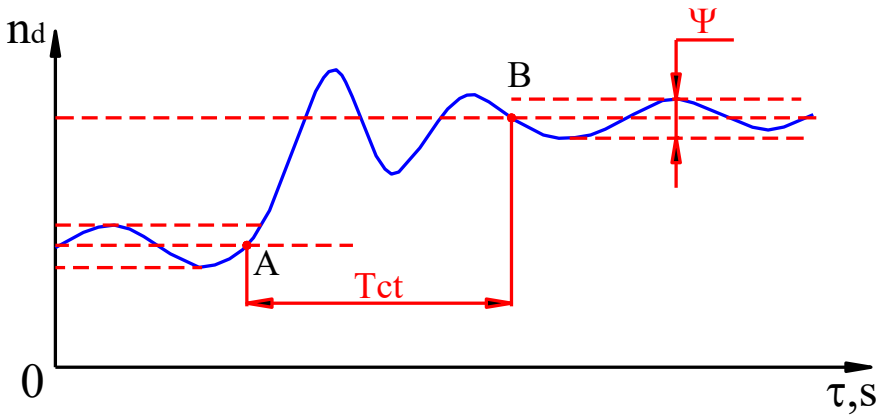

Fig. 2. Transient process of the engine during sudden load disengagement

2.2. Variation of Engine Operating Parameters During Load Engagement Process

This is a frequent working process for engines installed on transport vehicles or construction machinery. The process can be divided into three phases:

Phase 1 corresponds to the period of changing the fuel quantity supplied per cycle (Δg_{ct}).

Phase 2 is characterized by a rapid change in the engine's operating parameters and lasts until the rated speed is reached.

Phase 3 occurs with minor changes in parameters compared to the increase in engine speed (n_d).

The load engagement characteristic determines phase 1; Phase 2, which is shorter, is marked by rapid and significant variations in working parameters. Phase 3 differs from the previous two in that the parameters vary only slightly until the engine is fully warmed up and reaches a new steady-state condition. During load engagement (when the resisting torque increases), the fuel rack of the high-pressure pump moves quickly to increase the fuel quantity supplied per cycle. This movement is governed by the static and dynamic characteristics of the governor as well as

the high-pressure pump properties. In the initial stage of load engagement, engine speed decreases rapidly because the resisting torque exceeds the torque produced. The crankshaft speed drops sharply, causing the governor to move the fuel rack, thereby increasing fuel supply. At this stage, the fuel injection duration (in terms of crank angle) and the fuel injection advance angle (φ_{fs}) both decrease compared to their steady-state values. As a result, the combustion process tends to extend into the expansion stroke. Compared with steady-state conditions, the maximum pressure (P_z) and maximum pressure rise rate $(dp/d\varphi)_{max}$ decrease, leading to a deterioration of the indicated parameters of the cycle.

The variation characteristics of the operating parameters of large turbocharged engines mainly depend on the coordination between the fuel supply system and the air supply system. After load engagement, within a few operating cycles, the fuel quantity per cycle increases sharply; the governor's properties determine the magnitude of this increase. As fuel delivery rises, the air excess coefficient (α) decreases rapidly and reaches a minimum value, which significantly differs from that of the new steady-state condition. Because the rotational speed of the compressor-turbine rotor increases slowly due to its inertia, the air excess coefficient (α) continues to decrease rapidly. From the expression defining the air excess coefficient:

$$\alpha = G_k / L_o . g_{ct} \quad (2)$$

It can be seen that during a sudden load increase, (G_k) (air mass flow rate) does not change immediately, while g_{ct} (fuel quantity per cycle) increases, causing (α) to decrease. After some time, the crankshaft speed approaches the new steady-state value, while the turbine speed recovers more slowly. In the early stage, the exhaust gas pressure before the turbine exceeds the compressor outlet pressure (P_k), leading to backflow of exhaust gas into the intake manifold, which further reduces (α). Only later does the pressure return to normal. The minimum value of the air excess coefficient (α) occurs in the early stage of the transient process, negatively affecting the in-cylinder working process and deteriorating the indicated and effective performance parameters, thus reducing the engine's overall efficiency. The maximum combustion pressure in the working cycle becomes lower than the value corresponding to the steady-state mode. Applying a fuel delivery control mechanism based on the boost pressure is an effective measure to improve the indicated and effective parameters of turbocharged diesel engines.

3. Design and Fabrication of the Control System

3.1. Controller and Auxiliary Air Supply Device in Transient Mode

The components used for the automatic supplementary air supply system include a main and auxiliary microprocessor, various electronic components, a speed sensor, a fuel rack position sensor, an intake air flow sensor, a compressed air tank pressure sensor, and a solenoid valve for supplementary air injection. The selection of these components must ensure they can perform the required functions as mentioned above. The microprocessors must be compatible with both the sensors and the actuators. At the same time, all components should be readily available on the market and reasonably priced. The selected components are shown in Fig. 3.

The sensors used in this study have the following specifications:Inductive speed sensor: measuring range from 10 to 10,000 (rpm); output frequency 0 to 10 (kHz); installation distance 0.5 to 2 (mm); Displacement (position) sensor: stroke length 50 (mm); resolution 0.1 (mm); accuracy ±0.1 (mm); Intake manifold pressure sensor: pressure measurement range 20 to 250 (kPa); linear output voltage 0.5 to 4.5 (V); accuracy ±3%; Kármán-vortex type airflow sensor: airflow measurement range up to 5000 (L/min); output signal at no-load condition from 0.7 to 1.2 (V); under increased load, the output signal rises to 4–4.5 (V); accuracy ±2%.

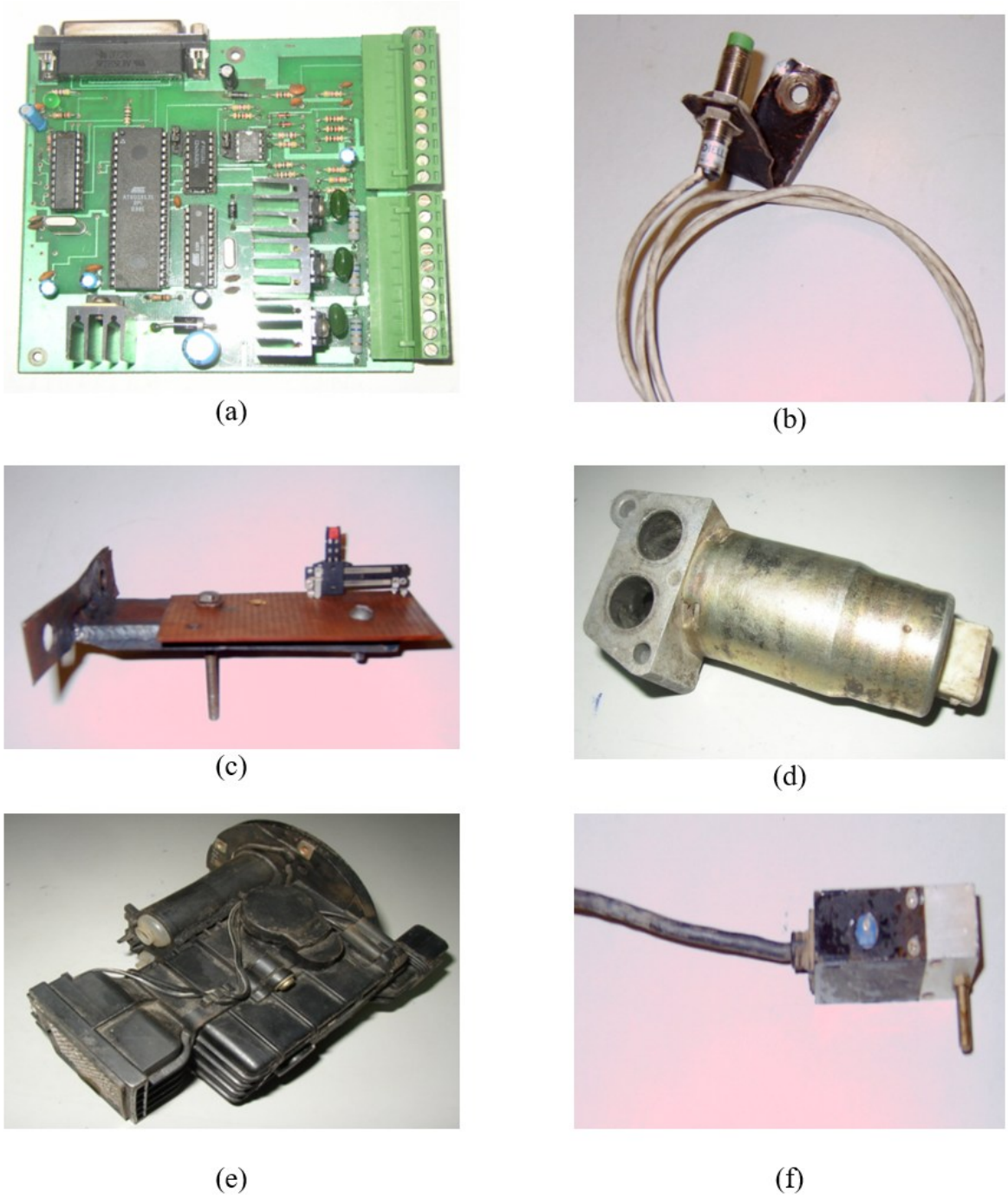

Fig. 3. Components used in the air supply control system include (a) Electronic Control Unit (ECU), (b) Speed Sensor, (c) Rack Position Sensor, (d) Additional Air Supply Valve, (e) Intake Air Flow Sensor, (f) Intake Air Pressure Sensor

3.2. Control Algorithm for Supplementary Air Supply

The algorithm diagram of the automatic supplementary air supply control system for the engine shown in Fig. 4 is explained as follows: Determine the change in fuel rack position (Δh_p); Compare the rate of change of (Δh_p) over time with the given (ψ_{hp}) value to determine the start time of the transition process; Determine the actual air flow value (G_{tt}) on the intake pipe. Each of these values corresponds to a crankshaft rotation value and a rack position value at the same time; Compare the actual air flow value (G_{tt}) with the sample air value G_{ct}; Calculate the amount of air that needs to be supplemented: $\Delta G = G_{ct} - G_{tt}$; Calculate the pressure difference before and after the

supplementary air supply solenoid valve: $\Delta P = P_2 – P_1$; Calculate the opening of the solenoid valve through the air flow values and the pressure difference at the valve port.

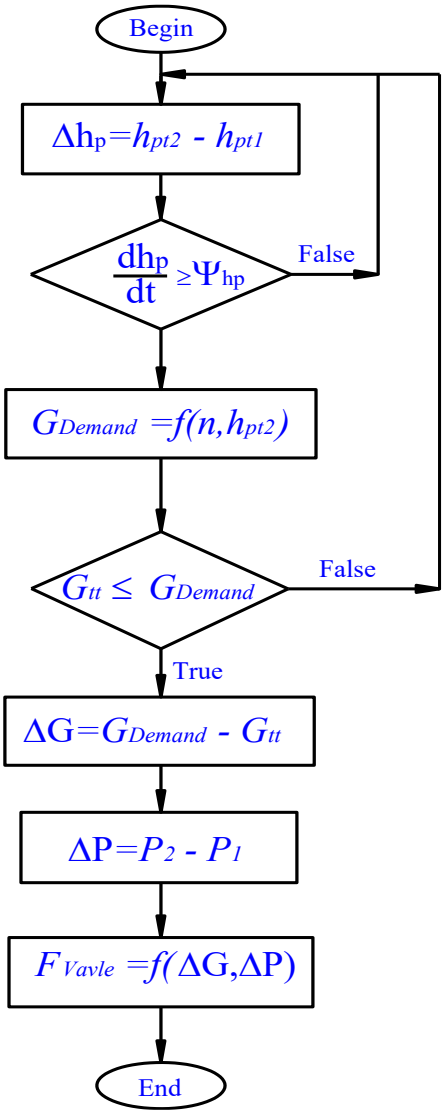

Fig. 4. Control Algorithm Diagram for Supplementary Air Supply

4. Experimental Evaluation

4.1. Experimental Setup and Equipment

The study was conducted using a four-stroke ISUZU 4BD1T diesel engine featuring a direct-injection combustion chamber and turbocharging by an exhaust gas turbine. The engine has four vertically arranged cylinders and employs a Bosh-type plunger high-pressure pump with a mechanical multi-mode governor. The maximum engine power is 78.3 kW at 2500 rpm, and the maximum engine speed is 2750 ± 50 rpm. The engine was mounted on an engine test bench with a maximum capacity of 73.5 kW and an electrical dynamometer speed range of 1500–3000 rpm. The test bench is equipped with sensors to measure engine speed, intake air pressure, and flow rate, fuel rack position, and fuel consumption.

The schematic diagram of the experimental setup for the automatic supplementary air supply system is shown in Fig. 5. The system consists of the following components: air tank capacity 100 dm^3; engine speed sensor, fuel rack position sensor, intake air flow sensor, and intake air pressure sensor; Electronic Control Unit (ECU) capable of communication with a PC; Solenoid valve for supplying supplementary air to the engine.

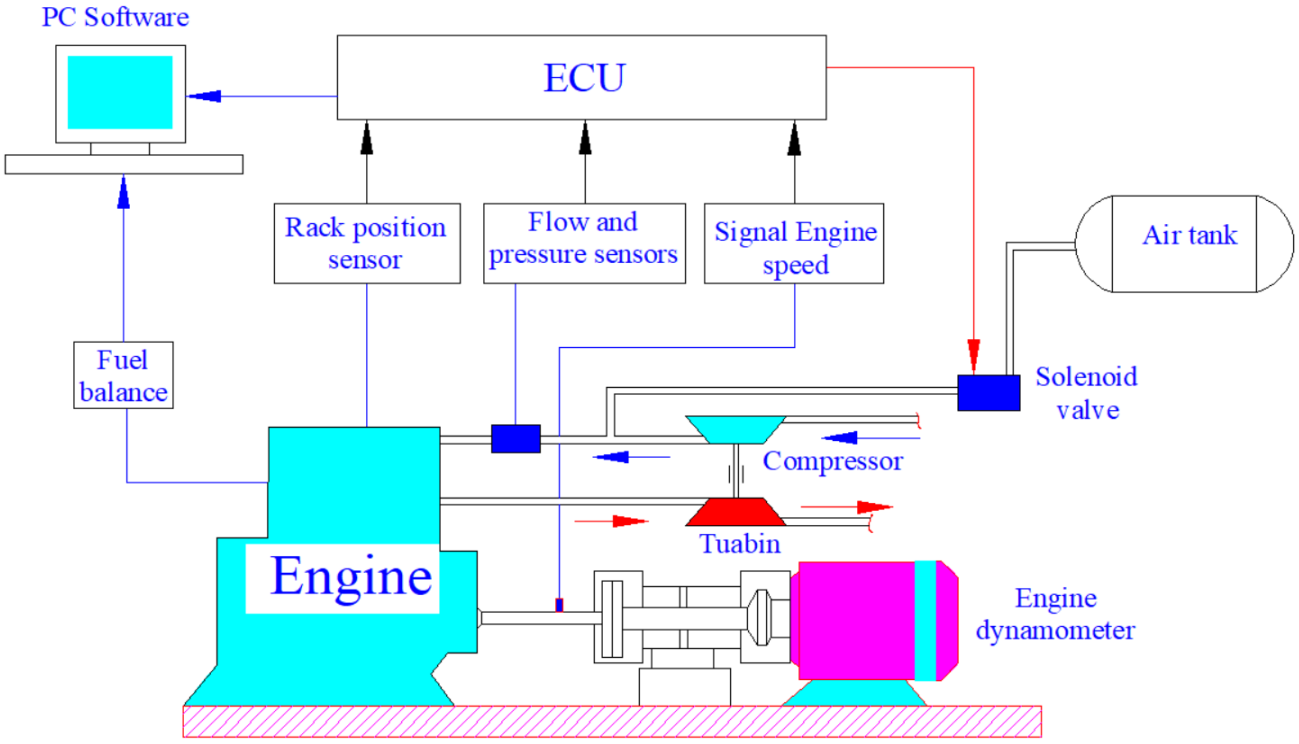

Fig. 5. Schematic Diagram of the Supplementary Air Supply System

4.2. Engine Testing Procedure on the Test Bench

4.2.1. Establishing the transient air-flow relationship as a function of engine speed and fuel-rack position

For each position (h_{pi}) of the fuel rack, there corresponds a specific value of fuel injected into the engine (G_{nli}). To ensure complete combustion of the fuel quantity (G_{nli}), the engine requires a corresponding amount of actual intake air (G_{cti}). With these two values unchanged, the engine will operate stably at a speed (n_{dci}). As analyzed and calculated in the previous chapters, during sudden load engagement, for the same values of fuel quantity (G_{nli}) and engine speed (n_{dci}), the actual intake air quantity (G_{tti}) is always less than the required theoretical air quantity (G_{cti}). Therefore, to accurately compensate for the amount of air needed and ensure complete fuel combustion, thereby improving the quality of the transient process, it is necessary to determine the difference: $\Delta G_i = G_{cti} - G_{tti}$

where:

G_{cti}: Required air quantity corresponding to steady-state operation

G_{tti}: Actual air quantity measured by the intake air flow sensor at any instant during transient operation

The value of (G_{cti}) is obtained from the relationship $G_{ct} = f(n_{dc};h_p)$, while G_{tti} is directly measured in real time.

The experimental process to find the relationship between the required flow $G_{ct} = f(n_{dc};h_p)$ was carried out with many measurements of (G_{ct}) corresponding to the fuel rack positions (the values of (G_{nl})) and the values of engine speed (n_{dc}) in stable modes, with a maximum travel of the rack h_{pmax} = 20mm. We obtained the relationship between the rack travel and engine speed as shown in Table 1.

The above data array is loaded into the main microprocessor AT90S8535 to determine (G_{ct}) during the supplementary air supply control process.

4.2.2. Determination of Fuel Rack Displacement Speed

During steady-state operation of the engine, the position of the fuel pump rack fluctuates around a stable value, depending on the uniformity of the governor. When the engine load changes, the rack

position also varies accordingly. Suppose the external load on the engine changes slightly or gradually. In that case, the engine operates with sufficient air supply, and the rack displacement speed remains smaller than or equal to a specific value (ψ_{hp}). However, if the load changes suddenly by a sufficiently large amount within a short time, the engine operates under an air-deficient condition, and the rack displacement speed increases, exceeding the threshold value (ψ_{hp}). Thus, the beginning of the transient process is identified at the moment when the rack displacement speed exceeds the set threshold (ψ_{hp}). The rack position sensor performs this task. Every small change in the rack position causes a corresponding change in the sensor's resistance, generating an analog signal sent to the main microprocessor. This signal serves as crucial information reflecting the change in engine load.

Experimental results determined the rack displacement speed as ψ_{hp} = 80 divisions/second (equivalent to 4 mm/s), as shown in Fig. 6.

Table 1. Supplementary Air Flow Rate as a Function of Fuel Rack Position and Engine Speed

Rack Displacement (h_p mm)	Required air flow rate G_{ct} corresponding to engine speed and fuel rack position (m^3/min)				
	1500 (rpm)	1800 (rpm)	2000 (rpm)	2250 (rpm)	2500 (rpm)
7	3.370	3.830	4.070	4.360	4.680
9	3.375	3.910	4.240	4.560	4.960
11	3.380	3.970	4.312	4.759	5.390
13	3.385	4.008	4.425	4.945	5.467
15	3.390	4.038	4.461	5.006	5.544
17	3.395	4.062	4.508	5.065	5.622
19	3.400	4.103	4.584	5.092	5.700

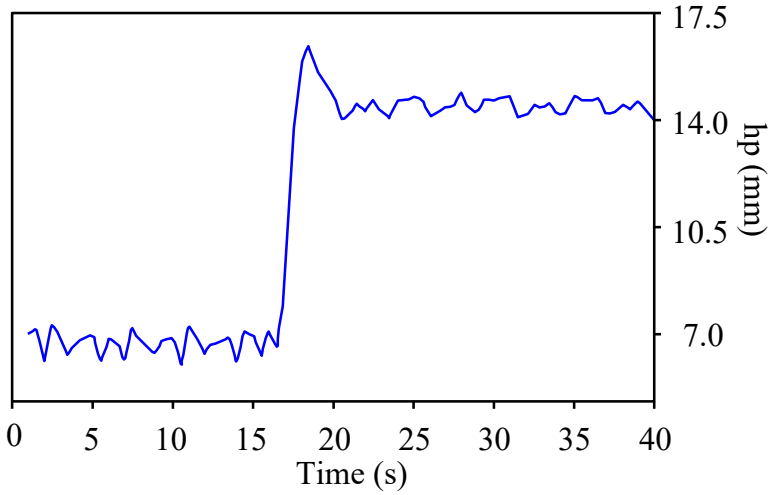

Fig. 6. Measured variation rate of fuel rack position (h_p) at 65% load

The value of 4 mm/s is loaded into the main microprocessor as a reference to determine the starting point of the engine's transient process.

4.2.3. Establishing the Valve-Opening Relationship and Selecting the Supplementary Air Supply Device

Relationship between Valve Opening and Variations in Air Flow and Pressure:

The supplementary air quantity supplied to the engine at an instant tit_iti during the transient load change is determined by the formula:

$$\Delta G_i = G_{bsi} = G_{cti} - G_{tti} \quad (3)$$

The airflow through the valve is determined from the continuity equation:

$$G_{bsi} = \mu . F_{valve} \sqrt{\frac{2\Delta p}{\rho_{kk}}} \quad (4)$$

The air flow through the valve is determined from the continuity/flow equation:

where:

ρ_{kk} - density of compressed air (kg/m³);

G_{bsi} - supplementary air flow required at time tit_iti (m³/s);

Δp - pressure difference before and after the valve (given in the original as kG/cm²).

For simplicity, the pipeline losses and the delay of the compressed air flow from the air tank to the solenoid valve are neglected, assuming that:

$$\Delta p = p_{air\ tank} - p_{intake\ manifold} \quad (5)$$

μ - flow coefficient: $\mu = \varphi_{td}.\varepsilon_{bd}$ (6)

φ_{td} – velocity coefficient, ranging from 0.8 ÷ 0.9; for air, φ_{td} = 0,9 is selected.

ε_{bd} = 0.97÷0.98 – contraction coefficient accounting for the flow constriction effect; in cases where the valve orifice area is much smaller than the valve body ε_{bd}= 0.98

From this, the solenoid valve orifice area is determined using the following formula:

$$F_{valve} = \frac{G_{bsi}}{\mu\sqrt{\frac{2\Delta p}{\rho_{kk}}}} \quad (7)$$

The relationship $F_{valve} = f(\Delta G; \Delta p)$ is preloaded into the main microprocessor to calculate the valve flow area at any given moment based on the values of ΔG and Δp.

Selection of the Flow Area of the Solenoid Valve for Supplementary Air Supply:

Table 2. Valve Opening Area According to Load and Air Flow Rate

F_{valve} *(mm²)*				
G_{BSmax}*(m³/s)*	65% Load	75% Load	85% Load	95% Load
$P_{air\ tank}$ (Mpa)	0.0270	0.0317	0.0350	0.0356
0.3	65.8 mm²	74.0 mm²	81.5 mm²	83.1 mm²
0.4	51.8 mm²	59.5 mm²	65.5 mm²	66.8 mm²
0.5	44.3 mm²	51.3 mm²	56.4 mm²	57.6 mm²
0.6	39.3 mm²	45.6 mm²	50.2 mm²	51.4 mm²

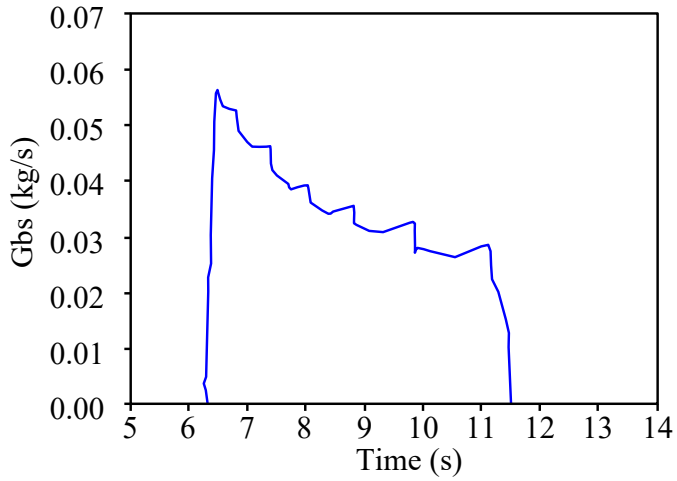

Fig. 7. Variation of supplementary air flow at 95% load

According to theoretical calculations, Table 2 below presents several values of the maximum valve flow area corresponding to different load engagement levels and various compressed air pressures in the air tank:

Based on the Table 2, it can be seen that selecting the idle valve from the electronic fuel injection system can meet the engine's supplementary air requirements. The valve has a diameter of 12 mm, with a maximum orifice area of 113.04 mm². The compressed air pressure in the air tank can be chosen between 0.3 and 0.6 MPa,

depending on the engine load level. In this experiment, since the load was only increased to 65%, a tank pressure of 0.3 MPa was selected. The volume of the independent compressed air tank is determined according to the maximum amount of supplementary air required by the engine. Theoretical calculations show that at the highest load (95%), the total supplementary air needed reaches a maximum of 0.1769 kg (equivalent to 136 dm³ under standard conditions). The variation of supplementary air supplied to the engine at 95% load is illustrated in Fig. 7.

During the supplementary air supply process, the independent compressor continuously supplies air to the compressed air tank. Therefore, a tank volume of 100 dm³ can be selected.

Experiment on Automatic Supplementary Air Supply for the Engine:

The engine load was varied experimentally by opening and closing the switches of the electric brake according to preset load levels on the test bench. This method is effective for creating sudden load changes on the engine. The intensity of the load change depends on the preset high or low load levels on the electric brake. To ensure safety for personnel and equipment, the sudden load tests in this experiment were conducted only at 65%, 55%, 50%, 40%, and 35% load levels.

The experiment was carried out multiple times under two conditions: Without supplementary air: The inlet of the solenoid valve was blocked. The results were recorded in data tables and graphs generated directly on the PC; With supplementary air: The inlet of the solenoid valve was opened. Based on the measured instantaneous air flow (G_{tti}) in the intake line, the ECU compared it with the required flow (G_{cti}) (corresponding to (G_{nli}) and (n_{dci}), determined the solenoid valve opening (valve orifice area F_{valve}), and, through the power stage, controlled the supplementary air supply to the engine.

4.3. Experimental Results

4.3.1. Criteria for Evaluating the Quality of the Load-Change Process

The study aimed to improve the operational parameters of a turbocharged diesel engine with an exhaust gas turbine, as described in the theoretical calculations and validated on the engine test bench. In the experimental context, it is necessary to define practical criteria for evaluating the effectiveness of the implemented control method. These criteria must not only reflect the intrinsic quality of the transient process but also be feasible for measurement under experimental conditions at an acceptable cost.

To assess the quality of the transient process, the following evaluation indicators were considered:

Transient Process Duration of the Engine (T_{ct}):

This is the time (measured in seconds) from the start of the transient process to the moment when the engine speed reaches the new steady state value. It is the most important indicator for evaluating the quality of the engine's transient response. (T_{ct}) reflects the adaptability of the turbine-compressor assembly and the stability of the governor operation in response to changes in engine load.

The (T_{ct}) value can be determined using an oscillograph during testing or from simulation results generated by the microprocessor when the automatic supplementary air supply system is connected to a computer. With the rapid development of information technology today, selecting an appropriate microprocessor installed on an electronic circuit to replace an oscilloscope not only provides accurate measurement results but also offers great convenience for data calculation and processing on a personal computer.

The relative change in engine speed is calculated based on the instantaneous engine speed compared to the rated speed:

$$\varphi = \frac{\omega - \omega_{dm}}{\omega_{dm}} \quad (8)$$

This is an important indicator to evaluate the degree of change in engine rotation when changing the load.

4.3.2. Experimental results

The measured results of the experiments with different loading levels are displayed on the PC screen as follows: nd (above) is the variation in engine speed, (h_p) (below) is the variation in rack position. Each graph shows two loading times: the first time without additional air supply; the second time with additional air supply. The results are shown in Fig. 8 and summarized in Table 3.

Table 3. Comparison of improvement results when experimenting with supplementary air supply to the engine

Load (%)	Mode	n_{max} (rpm)	n_{min} (rpm)	n_{od} (rpm)	Δn (rpm)	Δt (s)	Improvement
65	Normal	2502	2342	2379	160	3	–
	Transition	2502	2358	2379	144	2	Δt: 33.33%, Δn: 10%
55	Normal	2492	2347	2382	145	3	–
	Transition	2492	2363	2382	129	2.5	Δt: 16.66%, Δn: 24.13%
50	Normal	2393	2268	2329	125	2.5	–
	Transition	2393	2283	2329	110	1.5	Δt: 40%, Δn: 12%
40	Normal	2400	2271	2329	129	2	–
	Transition	2400	2282	2329	118	1.5	Δt: 25%, Δn: 8.5%
35	Normal	2409	2300	2338	38	1.5	–
	Transition	2409	2301	2338	37	1.5	No improvement

Notes:

Δt: reduction in withdrawal time compared to normal mode.

Δn: reduction in engine speed difference (n_{max} - n_{min}) compared to normal mode.

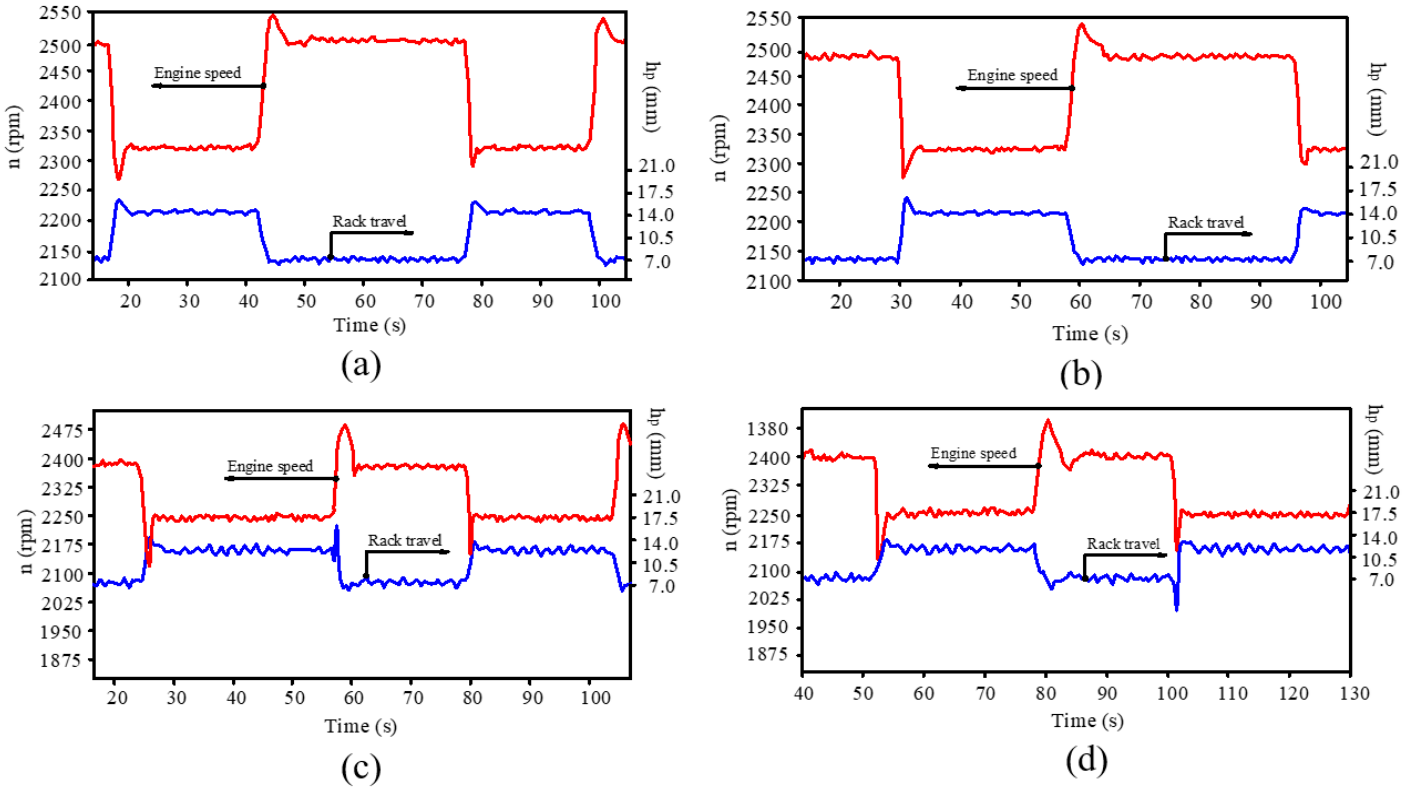

Fig. 8. Variation of (h_p) and (n_d) at operating conditions of (a) 65% load, (b) 55% load, (c) 50% load, (d) 40% load, (e) 35% load

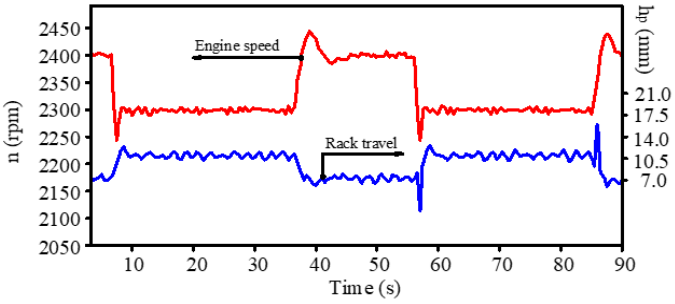

(e)

Fig. 8. (continued)

5. Discussion

The research results show that the air supply control system during the transient mode has demonstrated apparent effectiveness in improving the response and stability of the turbocharged diesel engine under various load conditions. Specifically, at medium and high loads (50÷65%), the engine stabilization time was significantly reduced by 16.6% to 40%, while the speed fluctuation (Δn) decreased by 8.5% to 24% compared with regular operation.

This indicates that the supplementary intake air control via the bypass line effectively reduced the turbocharger lag, maintained a more stable boost pressure, and minimized speed fluctuations during the transient period. At low load levels (35÷40%), the improvement was less significant due to the low boost pressure and intake airflow, which limited the impact of supplementary air control.

Overall, the experimental results confirm that the designed air supply controller successfully shortened the transient duration, reduced speed oscillations, and enhanced the operational stability of the engine, particularly effective in the medium to high load range. This contributes to improving the dynamic response of the turbocharging system and reducing emissions during transient operation.

6. Conclusion

The study successfully designed and fabricated an air supply controller for the transient mode of a turbocharged diesel engine, aiming to improve its response capability and speed stability during load changes. Two key parameters, engine speed and fuel rack position, were monitored, allowing accurate evaluation of transient characteristics under the available technological conditions in Vietnam.

Experimental results at five load levels showed that the transient time decreased from 3 seconds to 1.5÷2 seconds (an improvement of 16÷40%), while speed fluctuations (Δn) decreased by 8÷24% compared to regular operation. These results are consistent with theoretical calculations and previous studies, confirming that the supplementary air supply system operated effectively, reducing turbo lag and improving the operational stability of the engine.

Based on both theoretical and experimental findings, it can be concluded that the automatic air supply controller for transient conditions was successfully developed and operated stably, fulfilling the design objectives of enhancing the performance characteristics of a turbocharged diesel engine. The research outcomes provide an essential basis for refining the air control model of diesel engines under real operating conditions and open up prospects for wider applications in industrial and transportation engine systems in Vietnam.

References

[1] G. Wu, G. Feng, Y. Li, T. Ling, X. Peng, Z. Su, X. Zhao. (2024). A review of thermal energy management of diesel exhaust after-treatment systems technology and efficiency enhancement approaches. *Energies*, 17(3), 584. https://doi.org/10.3390/en17030584

[2] N.V. Tuan, N.P. Truong, N.T. Nghia. (2024).

Evaluate the effects of biodiesel fuel sources on Common Rail engine performance and emissions. *RASĀYAN Journal of Chemistry*, 17(4), 1436-1443. http://doi.org/10.31788/RJC.2024.1748845

[3] A.G. Olabi, D. Maizak, T. Wilberforce. (2020). Review of the regulations and techniques to eliminate toxic emissions from diesel engine cars. *Science of The Total Environment*, 748, 141249.https://doi.org/10.1016/j.scitotenv.2020.141249

[4] N.V. Tuan, N.X. Khoa, N.T. Nghia. (2025). A neural network approach on forecasting the engine emission using biodiesel fuel from fish oil based on injection pressure and engine operating parameters. *Engineering Applications of Artificial Intelligence*, 162(Part D), 112628. https://doi.org/10.1016/j.engappai.2025.112628

[5] Z. Gao, Y. Xiao, J. Mao, L. Zhou, X. Li, Z. Li. (2024). Optimization of second-generation biodiesel blends to enhance diesel engine performance and reduce pollutant emissions. *Energies*, 17(23), 5829. https://doi.org/10.3390/en17235829

[6] I. Bahiuddin, S.A. Mazlan, F. Imaduddin, Ubaidillah. (2017). A new control-oriented transient model of variable geometry turbocharger. *Energy*, 125, 297-312. https://doi.org/10.1016/j.energy.2017.02.123

[7] Q. Zhu, A. Kumar, E. Vorwerk, R. Prucka. (2025). Airpath control of opposed piston two-stroke diesel engines using model predictive control. *IEEE Transactions on Control Systems Technology*, 34(2), 601-616. https://doi.org/10.1109/TCST.2025.3624424

[8] N. Jin, W. Long, C. Xie, H. Tian. (2025). After-treatment technologies for emissions of low-carbon fuel internal combustion engines: Current status and prospects. *Energies*, 18(15), 4063. https://doi.org/10.3390/en18154063

[9] J. Pennington, P. Puzinauskas, J. Cook. (2021). Simultaneous control optimization of variable-geometry turbocharger and high pressure EGR on a medium duty diesel engine. *SAE Technical Paper*, 2021-01-1178. https://doi.org/10.4271/2021-01-1178

[10] E.R. Gelso, J. Dahl. (2016). Air-path control of a heavy-duty EGR-VGT diesel engine. *IFAC-PapersOnLine*, 49(11), 589-595. https://doi.org/10.1016/j.ifacol.2016.08.086

[11] C.D. Rakopoulos, C.N. Michos, E.G. Giakoumis. (2005). Study of the transient behavior of turbocharged diesel engines including compressor surging using a linearized quasi-steady analysis. *SAE Technical Paper*, 2005-01-0225. https://doi.org/10.4271/2005-01-0225

[12] W. Gu, W. Su. (2023). Study on the effects of exhaust gas recirculation and fuel injection strategy on transient process performance of diesel engines. *Sustainability*, 15(16), 12403. https://doi.org/10.3390/su151612403

[13] S. Kim, S. Choi, H. Jin. (2016). Pressure model based coordinated control of VGT and dual-loop EGR in a diesel engine air-path system. *International Journal of Automotive Technology*, 17(2), 193-203. https://doi.org/10.1007/s12239-016-0019-8

[14] B. Hu, J. Li, S. Li, J. Yang. (2019). A hybrid end-to-end control strategy combining dueling deep Q-network and PID for transient boost control of a diesel engine with variable geometry turbocharger and cooled EGR. *Energies*, 12(19), 3739. https://doi.org/10.3390/en12193739

[15] A. Norouzi, H. Heidarifar, M. Shahbakhti, C.R. Koch, H. Borhan. (2021). Model predictive control of internal combustion engines: A review and future directions. *Energies*, 14(19), 6251. https://doi.org/10.3390/en14196251

[16] S. Larguech, S. Aloui, O. Pagès, A. El Hajjaji, A. Chaari. (2019). Robust adaptive controller for the diesel engine air path with input saturation. *International Journal of Control, Automation and Systems*, 17, 2541-2549. https://doi.org/10.1007/s12555-018-0300-x

[17] C. Gamache, M.V. Nieuwstadt, J. Martz, G. Zhu. (2024). LQTI boost pressure and EGR rate control of a diesel air charge system with eBoost assistance. *International Journal of Engine Research*, 25(9), 1659-1670. https://doi.org/10.1177/14680874241241364

[18] S.M. Saad, A. Rummana. (2024). Transient response of turbocharged compression ignition engine under different load conditions. *SAE International Journal of Engines*, 17(1), 03-17-01-0005, 73-102. https://doi.org/10.4271/03-17-01-0005

[19] F. Zhang, Z. Wang, J. Tian, L. Li, K. Yu, K. He. (2020). Effect of EGR and fuel injection strategies on the heavy-duty diesel engine emission performance under transient operation. *Energies*, 13(3), 566. https://doi.org/10.3390/en13030566

[20] J. Galindo, H. Climent, J. de la Morena, D. González-Domínguez, S. Guilain. (2023). Assessment of air management strategies to improve the transient response of advanced gasoline engines operating under high EGR conditions. *Energy*, 262(Part B), 125586. https://doi.org/10.1016/j.energy.2022.125586

[21] B. Oh, M. Lee, Y. Park, J. Sohn, J. Won, M. Sunwoo. (2013). VGT and EGR control of common-rail diesel engines using an artificial neural network. *Journal of Engineering for Gas Turbines and Power*, 135(1), 012801. https://doi.org/10.1115/1.4007541

[22] H.A. Al-Hamzawi, A.S. Al Sailawi, R.Z. Homod, H.A. Kadhim, H.I. Mohammed, M.A. Al-Shareeda. (2025). Machine learning-enhanced optimization of exhaust gas recirculation strategies for superior diesel engine performance and emissions control: A synergistic experimental and computational study. *International Journal of Hydrogen Energy*, 169, 151184. https://doi.org/10.1016/j.ijhydene.2025.151184

[23] Q. Peng, D. Huo, C.M. Hall. (2022). Neural network-based air handling control for modern diesel engines. *Proceedings of the Institution of Mechanical Engineers, Part D: Journal of Automobile Engineering*, 237(5), 1113-1130. https://doi.org/10.1177/09544070221083367

[24] C. Gurel, E. Ozmen, M. Yilmaz, D. Aydin, K. Koprubasi. (2017). Multi-objective optimization of transient air–fuel ratio limitation of a diesel engine using DoE based Pareto-optimal approach. *SAE International Journal of Commercial Vehicles*, 10(1), 299-307. https://doi.org/10.4271/2017-01-0587

[25] Y. Han, L. Zhang, Z. Liu, J. Tian. (2016). Investigation of transient deterioration mechanism and improved method for turbocharged diesel engine. *Energy*, 116(Part 1), 250-264. https://doi.org/10.1016/j.energy.2016.09.088